IEEE Photonics Journal
An IEEE Photonics Society Publication

Open Access

High-Power Femtosecond Pulse Generation From an All-Fiber Er-Doped Chirped Pulse Amplification System

Volume 12, Number 2, April 2020

Rongling Wei
Mengmeng Wang
Zexiu Zhu
Weiyu Lai
Peiguang Yan
Shuangchen Ruan
Jinzhang Wang
Zhipei Sun
Tawfique Hasan

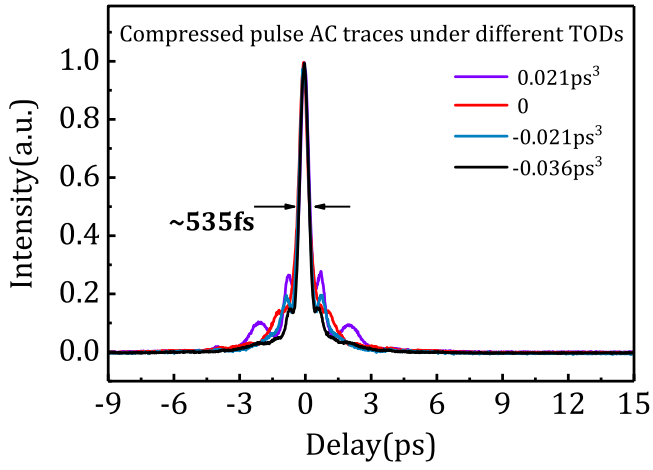

DOI: 10.1109/JPHOT.2020.2979870

High-Power Femtosecond Pulse Generation From an All-Fiber Er-Doped Chirped Pulse Amplification System

Rongling Wei,[1] Mengmeng Wang,[1] Zexiu Zhu,[1] Weiyu Lai,[1] Peiguang Yan,[1] Shuangchen Ruan,[1] Jinzhang Wang,[1] Zhipei Sun,[2,3] and Tawfique Hasan[4]

[1]Shenzhen Key Laboratory of Laser Engineering, College of Physics and Optoelectronic Engineering, Shenzhen University, Shenzhen 518060, China
[2]Department of Electronics and Nanoengineering, Aalto University, Aalto FI-00076, Finland
[3]QTF Centre of Excellence, Department of Applied Physics, Aalto University, Aalto FI-00076, Finland
[4]Cambridge Graphene Centre, University of Cambridge, Cambridge CB3 0FA, U.K.

DOI:10.1109/JPHOT.2020.2979870

Manuscript received December 19, 2019; revised February 29, 2020; accepted March 7, 2020. Date of publication March 10, 2020; date of current version March 24, 2020. This work was supported in part by National Natural Science Foundation of China (NSFC) under Grants 61605122 and 61775146 in part by Shenzhen Science and Technology Innovation Commission Program under Grant JCYJ20180305125335271 in part by China Postdoctoral Science Foundation under Grant 2018M643371 in part by Academy of Finland under Grants 276376, 295777, 312297, and 314810 in part by Academy of Finland Flagship Programmer under Grant 320167, PREIN, in part by the European Union's Horizon 2020 research and innovation program 290 under Grants 820423, S2QUIP. (Rongling Wei and Mengmeng Wang contributed equally to this work.) Corresponding authors: Peiguang Yan; Jinzhang Wang (e-mail: yanpg@szu.edu.cn; jzwang@szu.edu.cn).

Abstract: We demonstrate a compact all-fiber Er-doped chirped pulse amplification (CPA) system that can produce ~344 fs pulses with an average power of up to 1.02 W and a repetition rate of 40.6 MHz at 1.56 μm (corresponding to an energy of 25.1 nJ). The pulse compressor in the CPA system is based on a hollow core photonic crystal fiber which is directly butt-coupled to the silica fiber. A mismatched negative third-order dispersion is used to compensate the accumulated nonlinear phase shift in the amplification process for the first time, resulting in the generation of sub-400 fs pulses from an all-fiber Watt-level Er-doped CPA system. Our system architecture offers a possibility for ultrashort pulse generation from all-fiber Er-doped CPA lasers.

Index Terms: Fiber optics amplifiers and oscillators, ultrafast lasers, pulse compression, chirped pulse amplification.

1. Introduction

Over the past few decades, high-power femtosecond fiber lasers are of great interest for many scientific and industrial applications, due to their compact footprint, freedom from misalignment, environmental reliability and high beam quality. Their successful applications include ultrafast spectroscopy, material processing, and biomedical applications [1]–[3]. Among them, fiber lasers operating at 1.55 μm region are widely developed not only because of the availability of relatively cheap and mature telecom components, making the systems much more cost-effective than other laser sources, but also due to several charming applications, e.g., Si waveguide writing [4] and

corneal surgery [5]. Further, extending their output wavelength to ∼780 nm via second harmonic generation offers a great potential to replace commercial Ti: Sapphire lasers which are usually pumped by expensive green light sources.

Although femtosecond pulses at 1.55 μm are comparably easy to achieve from mode-locked Er fiber lasers [6]–[10], their power scaling ability and pulse fidelity are strongly limited by the fiber nonlinearity. A straightforward method to overcome these limitations is to use well-known chirped-pulse amplification (CPA) technique which was first proposed by Strickland and Mourou [11]. The typical processing of the CPA technique is that low energy pulses broadened by a dispersive element (e.g., a dispersion compensating fiber (DCF) or a grating pair) are significantly amplified in a high gain medium with reduced optical nonlinearities, and after that, the amplified pulses are compressed in a dispersive element with opposite dispersion. So far, the grating pair becomes a preferred option as a compressor in fiber-based sources due to its low nonlinearities. Building on this concept, Er-doped CPA fiber systems have been widely reported. They can produce pulses with Watt-level average power with pulse energy scaled either to several tens of nJ level (without a pulse picker) [12], [13] or to μJ level (with a pulse picker) [14]–[17]. Thus far, the shortest pulse duration from a Watt-level CPA Er fiber system is 175 fs [18], while the highest energy is 0.9 mJ [19]. However, the aforementioned systems included bulk optics, such as grating pairs for pulse compression and other optical elements for pump and signal light coupling, therefore, eliminating the benefits of the all-fiber format.

In order to construct an all-fiber based system, the pulse compressor could be realized by a hollow-core photonic crystal fiber (HC-PCF) instead of a bulk grating pair. Light propagating inside the HC-PCF is mainly confined to the hollow core (i.e., air-core) through diffraction from surrounded air holes rather than the traditional total internal reflection [20]. As a consequence, in addition to the advantage of the fiber flexibility, the HC-PCF manifests much lower (∼1000 times lower) optical nonlinear coefficient than traditional silica fibers, accordingly, capable of supporting much higher peak power [21]. Due to the negligible material dispersion in air-core, the dispersion of HC-PCF is dominated by waveguide dispersion, which has strong wavelength dependence and can increase from highly negative to highly positive in its transmission band. Such HC-PCF with controllable dispersion is hence quite suitable for intra-cavity dispersion compensation [22] and pulse compression in all-fiber CPA systems [21], [23], [24]. Imeshev *et al.* [25] reported on the generation of 570 fs, 310 nJ pulses at an average power of 155 mW from an Er CPA fiber system based on a 9.3-m long HC-PCF. The shortest pulse duration reported from an HC-PCF based Er CPA system is 440 fs, where the pulse energy is 21 nJ and the average power is ∼1 W [26]. However, these two fiber laser systems include free space bulk optics to couple light into the HC-PCF and gain fiber. To date, truly all-fiberized Er CPA systems realized by directly splicing the HC-PCF to silica fiber were demonstrated by C. J. S. de Matos *et al.* [27], [28]. However, the pulse duration is about 1 ps, not suitable for applications requiring ultrashort pulses.

In this letter, we demonstrate an entirely fiberized Er-doped CPA system based on a butt-coupled HC-PCF. No bulk optics are employed in the cavity. Unlike traditional fiber CPA systems which typically require both the group delay dispersion (GDD) and the third-order dispersion (TOD) compensation, our CPA system has a large negative uncompensated TOD (-0.041 ps^3) which can be used to compensate the accumulated nonlinearities in the amplifier, resulting in a pulse with relative low pedestal. The system generates 25.1 nJ, 344-fs pulses at the average power of 1.02 W. This is the first demonstration of fiber nonlinearities' compensation by negative TOD at 1.55 μm, resulting in the generation of shortest pulse duration from an all-fiber Er CPA system with Watt-level average power.

2. Chromatic Dispersion Measurements

Proper dispersion compensation is a key procedure in the CPA fiber systems. The GDD coefficient (β_2) and TOD coefficient (β_3) of different fibers used here are measured with a well-known white-light interferometry technique, with the setup similar to that of Refs. [29], [30]. In our experiment, we utilize a homemade broadband source as the white-light source with a 20-dB bandwidth of

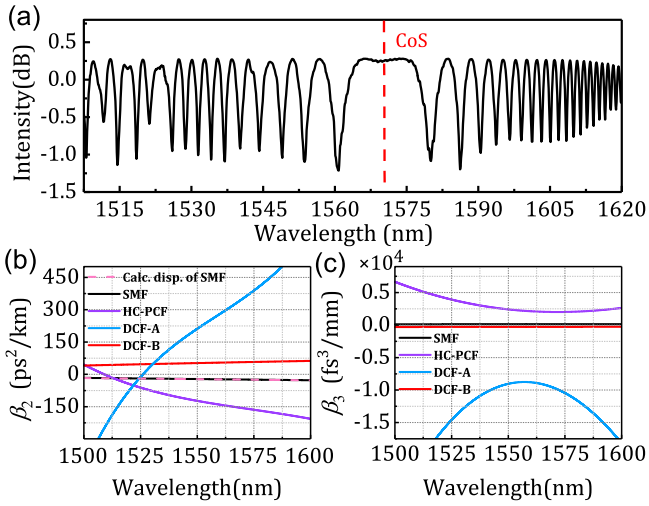

Fig. 1. (a) An exemplary spectral interferogram. (b) β_2 and (c) β_3 of different fibers as a function of wavelength.

$\sim$104 nm. Figure 1(a) presents an exemplary spectral interferogram based on a piece of DCF. The spectral phase could be extracted from the interferogram as the phase shift between the adjacent peak and valley is π, while the phase reaches maximum or minimum (depending on the sign of β_2) at the center of symmetry (CoS) [31]. Numerical differentiation of the spectral phase profile is then carried out to derive the GDD and TOD. To examine the accuracy of our measurement, a piece of standard single mode fiber (SMF-28e, Corning) is measured. The measured dispersion coincides well with the calculated results based on a dispersion formula offered by Corning (see Fig. 1(b)), confirming the reliability of our measurement.

Conventional wisdom suggests that the TOD will degrade the fidelity of temporal pulse. However, it has been demonstrated that the TOD can be used to compensate the nonlinear phase shift accumulated by a pulse amplified in a gain fiber [32]–[34]. This results in the generation of higher quality pulses (i.e., shorter pulse duration and high peak power), compared to that of a same CPA system in the absence of TOD. Although a numerical model based on symmetrical gain spectrum reveals that such compensation is independent of the sign of the residual TOD [33], the real experiments could be different as most of the ultrafast lasers don't work at the center of gain spectrum and present asymmetrical spectral profile. In that case, the spectral phase produced by the SPM is asymmetrical too. Thus, in order to qualitatively investigate the influence of TOD on the pulse quality in the CPA system, we employ two kinds of DCFs with different dispersion slopes (β_3/β_2), which will be marked as DCF-A (a custom product from YOFC Ltd.) and DCF-B (Thorlabs, DCF38) in the following context. By intentionally assembling two DCFs, we can achieve a fixed GDD with variable TOD. The measured β_2 and β_3 of different fibers are shown in Figs. 1(b) and 1(c). Their corresponding values at 1560 nm are summarized in Table 1. It should be noted that we are unable to measure the dispersion properties of Er gain fibers due to their large absorption at 1.55 μm. However, our EDFs have relatively small lengths, implying that they play a comparably small role in the total cavity dispersion.

3. Experimental Setup and Results

Figure 2 illustrates the experimental setup, which consists of a fiber oscillator and a two-stage amplifier. The fiber oscillator is mode-locked by a carbon nanotube saturable absorber (CNT-SA). Our oscillator exhibits a high self-starting mode-locking capability as a result of our reliable CNT-SA [6]. The cavity length is $\sim$5 m, corresponding to a fundamental pulse repetition rate of $\sim$40.6 MHz.

TABLE 1
The β_2 and β_3 of Different Fibers at 1560 nm

Fiber type	β_2 (ps^2/km)	β_3 (fs/mm)	β_3/β_2 (fs)
SMF-28e	-22.7	130	-5.73
HC-PCF	-140	2137	-15.26
DCF-A	290	-8798	-30.87
DCF-B	54.6	-271	-4.96

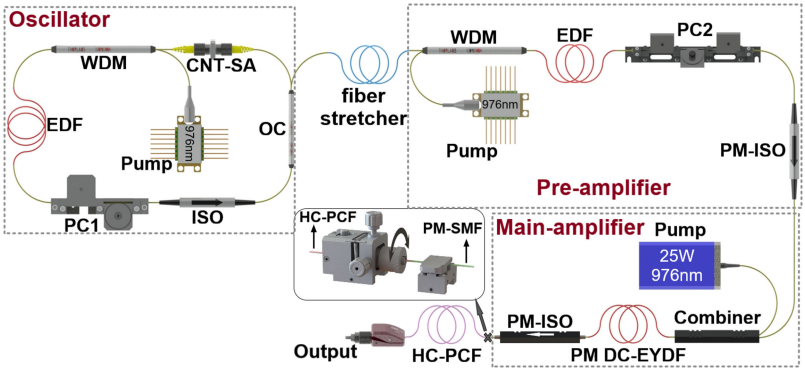

Fig. 2. Experimental setup of the Er CPA system. CNT-SA, Carbon nanotube saturable absorber; EDF, Er-doped fiber; WDM, wavelength division multiplexer; PM, polarization-maintaining; ISO, isolator; PC, polarization controller; DC-EYDF, double-clad erbium/ytterbium co-doped fiber; and HC-PCF, hollow-core photonic crystal fiber.

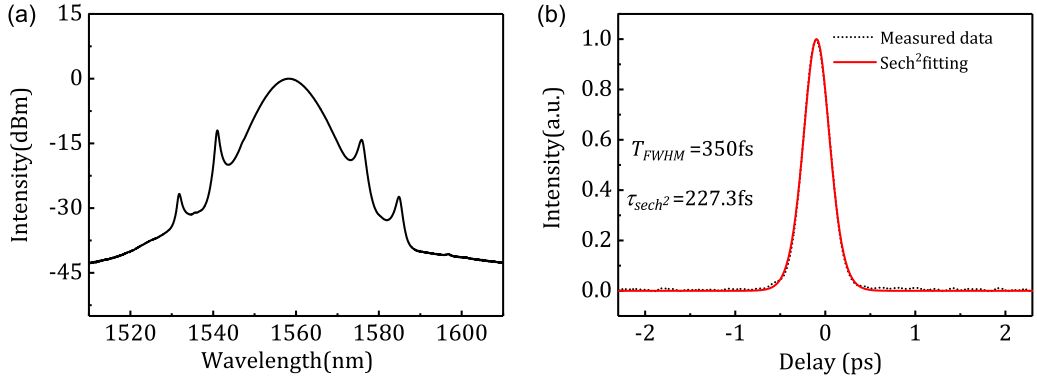

Fig. 3. (a) The oscillator spectrum. (b) The measured AC trace.

At the pump power of 110 mW, the average output power is 4.67 mW. Figure 3(a) shows the output spectrum, which is centered at 1558.4 nm and has an FWHM bandwidth of 11.4 nm. The clear Kelly sidebands indicate that the oscillator operates at soliton mode-locking regime. The autocorrelation (AC) trace is well fitted by a sech^2 shape with 350 fs width (see Fig. 3(b)). This gives a pulse duration of 227.3 fs at a time-bandwidth product (TBP) of 0.32, close to the transform limit of 223 fs.

The seed pulse is sent to a pulse stretcher with a stretching ratio of ∼100 and is stretched to ∼23 ps. Here, the pulse stretcher can have several types as explained later. The power is decreased to ∼1.8 mW due to the large splicing losses between the custom DCF and SMF caused

by the mismatch of their mode-filed diameters (∼4.0 and ∼10.4 μm, respectively) at 1.55 μm. After that, the stretched pulse is pre-amplified to ∼84 mW through a 3-m long Er-doped fiber (EDF, Fiber-core I25) pumped by a 976 nm single-mode laser diode (LD). A low-power polarization-maintaining (PM) isolator combining with a polarization controller (PC) is placed after the pre-amplifier to convert the polarized state of the signal into linear polarization. The main-amplifier is based on a 1.8-m long PM double-cladding Er/Yb co-doped fiber (DC-EYDF, CorActive, DC-EY-10/128-PM) which is forward-pumped by a 25 W, 976 nm multi-mode LD through a customized PM combiner. A high-power PM isolator is spliced to the output of the main-amplifier to block the residual pump light and any parasitic back-reflections. This is particularly important as only a little back-reflection light would be significantly increased in the last amplifier stage, leading to irreversible damage of those optical components with low damage threshold. The fiber pigtails made by PM-SMF (Nufern, PM1550-XP) of this isolator are as short as 25 cm, enabling to reduce detrimental nonlinear effects. The total length of passive fibers in the two stage amplifiers is around 7 m and the last amplifier stage is based on PM fibers to improve the laser stability. Finally, a 16-m HC-PCF (NKT, HC-1550-02) is used as a pulse compressor, with a mode filed diameter of ∼9 μm at 1550 nm, comparable to that of PM-SMF (∼10.1 μm). Therefore, we directly butt-couple the HC-PCF to the PM-SMF (see the inset of Fig. 2), resulting in an acceptable coupling efficiency of ∼43%. Here, the large coupling loss could be due to the absorption caused by the air contamination in the hollow core as our HC-PCF is exposed to the air circumstance for more than one year without any protection. The absorption loss is measured to be ∼28% by using the cut-back method. Moreover, no thermal degradations could be observed during the amplification. The overall system is made of all-fiberized components, without any free space bulk optics, and can output linearly polarized pulses. It should be noted that the HC-PCF presents considerable birefringence which will split the pulse into two orthogonal polarization pulses propagating with different group velocities [26]. The PM output feature of the amplifier is therefore capable of eliminating the polarization mode dispersion effect by aligning the fast axes of the HC-PCF and PM-SMF. This is realized by continuously rotating the fiber holder of HC-PCF until two side peaks observed in the AC trace have vanished in our experiment. Finally, more than 20 dB extinction ratio could be obtained.

As mentioned above, the mismatched TOD compensation in a CPA fiber system would be the benefit of high-quality pulse generation. However, this is only reported at 1 μm region [32], [33], [35], making related studies on 1.55 μm region highly desirable. We, therefore, investigate four types of pulse stretchers with the same GDDs and different TODs. They are based on a 50-m DCF-B, a 3-m DCF-A plus 28-m DCF-B, a 5.8-m DCF-A plus 16-m DCF-B, and an 8-m DCF-A, in combination with a variable piece of SMF for fine GDD tuning, corresponding to the net TODs of 0.021 ps^3, ∼0, $-$0.021 ps^3, and $-$0.036 ps^3, respectively. Note that the additional TODs of those fibers (e.g., SMF and Er fibers) between the stretcher and compressor are neglected since they are much smaller than that of DCF and HC-PCF. Figures 4(a) and 4(b) show the four AC traces after the HC-PCF compression at the output power of ∼0.5 W and ∼1 W, respectively. All these traces are recorded when the AC peak reaches a maximum. Apparently, a negative TOD is much preferred over the positive value for reducing the pulse pedestal (accordingly, increasing the peak power), and a minimum pedestal is reached at a large negative TOD (-0.036 ps^3). It is in contrast to that of Refs. [32], [33], where large positive values are used to compensate the SPM-induced nonlinear spectral phase at 1 μm. This could be attributed to the different gain spectra at 1.55 μm and 1.0 μm, which play a large role in the SPM. In particular, the central wavelength of our laser is 1.56 μm, having a 30-nm shift away from the emission peak (∼1.53 μm) of our Er gain fibers. A similar trend that exhibits lower pedestal in the presence of larger negative TOD, could be obtained by replacing the HC-PCF compressor with a diffraction gating pair (940 lines/mm, LightSmyth), as shown in the insets of Fig. 4(a) and 4(b). Only two traces are presented here for clear observation. Moreover, small pedestals far away from the central peak under high output power could be observed for all stretchers (see Fig. 4(a) and 4(b)). This is due to the excessive nonlinear phase shift resulting from a relatively small pulse stretching ratio (∼100). On the other hand, due to the SPM compensation of TOD mismatch, the FWHM widths of AC traces decrease from ∼535 to ∼500 fs when the output power increases from 0.5 to 1.0 W. In fact, the pulse duration first decreases to a minimum and

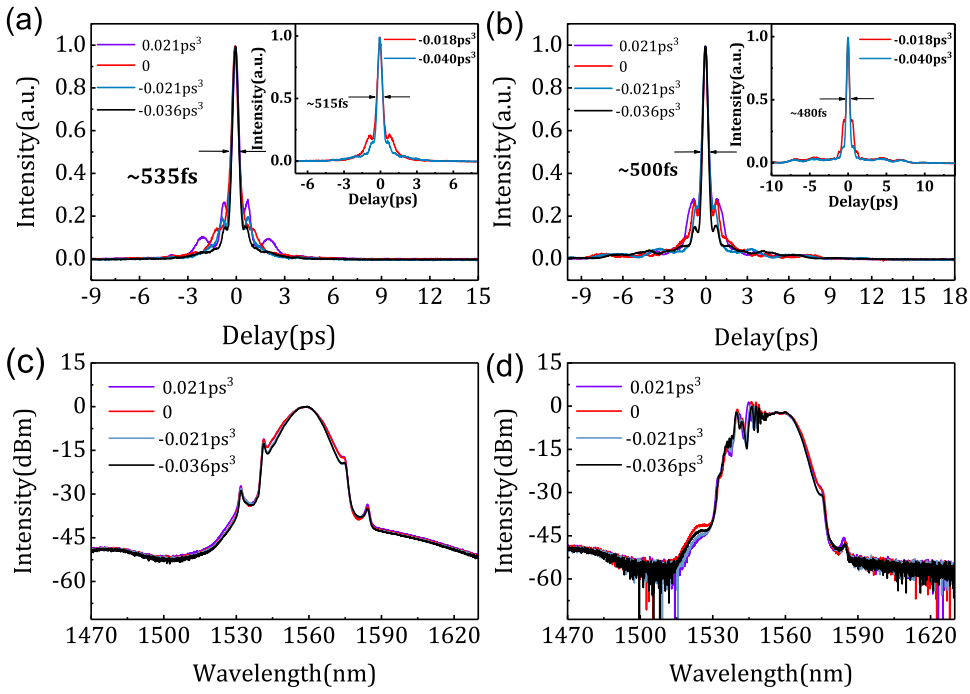

Fig. 4. (a and b) The AC traces of output pulse based on compression in HC-PCF with different net TODs at the output power of ~0.5 W and ~1.0 W. The insets in (a) and (b) give the AC traces based on a grating pair compressor with the power before the compressor same to that of HC-PCF. (c and d) The optical spectra before and after the main amplifier that correspond to the case in (b).

then increases when the pump power is increasing in our experiment, which is a typical signature of TOD/SPM compensation [33], [35]. Besides, the corresponding spectra before (Fig. 4(c)) and after (Fig. 4(d)) the main amplifier are also recorded when we measure the four AC traces of Fig. 4(b). No significant differences are observed before the main amplifier. The slightly different modulation periods on the spectra (Fig. 4(d)) after the amplifier might be due to the TOD/SPM compensation.

By further optimizing the TOD and the seed pulse power, a shortest pulse with the lowest pedestal could be achieved when the stretcher is based on a ~8.5 m DCF-A, corresponding to a net TOD of -0.041 ps^3. The average output power is ~1.02 W, corresponding to a pulse energy of 25.1 nJ. The calculated accumulative nonlinear phase shift (i.e., B-integral) is ~2.05. Figure 5(a) presents the output spectra before and after the HC-PCF compressor. The corresponding effective spectral widths are 15.8 and 13.8 nm, respectively. Slightly difference is due to the absorption of the HC-PCF. However, no significant changes in the spectrum can be observed, owing to the air-guidance properties of the compressor. The spectrum oscillation is a result of SPM. The small peak appeared on the left side of the spectrum might be caused by the ASE or Kelly sideband. The measured compressed AC trace is listed in Fig. 5(b). Assuming a gaussian pulse profile, the pulse has a duration of ~344 fs with a deconvolution factor of 0.707. The transform-limited (TL) pulse according to the pulse spectrum is also illustrated in the inset of Fig. 5(b), giving a TL duration of 232 fs. This is close to the pulse width of the oscillator, confirming that the gain narrowing effect could be compensated by the SPM. However, due to the incompletely uncompensated SPM effect, the dechirped pulse is longer than the TL pulse. Further increasing the pump power or the net TOD would lead to wider pulse duration, as well as a larger pedestal. Nevertheless, a much higher power could be expected if a much larger stretching ratio (e.g., ~1000 times) is used to decrease the excessive nonlinearity during the amplification. Although the stretching ratio could be increased by using a seed pulse operated at stretched-pulse regime which typically has a much wider spectral

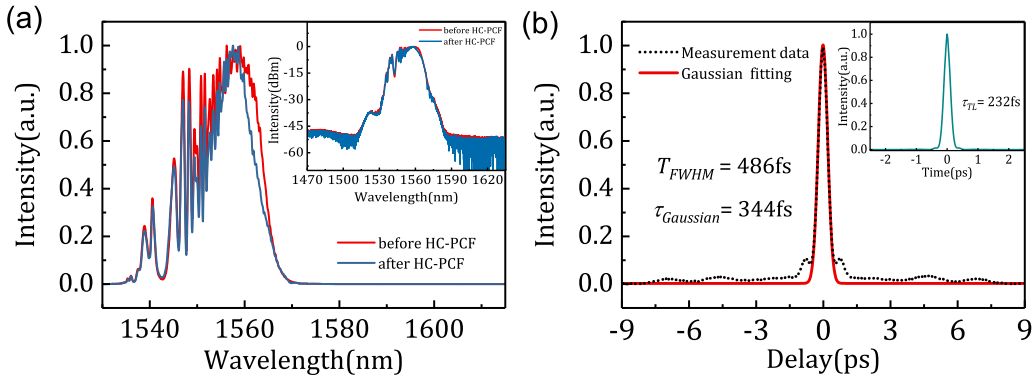

Fig. 5. (a) The measured spectra before and after the HC-PCF. Inset: The corresponding spectra on the semi-log scale. (b) The measured AC trace along with a gaussian profile fit. Inset: The calculated TL pulse.

bandwidth than that of soliton pulse, it's quite difficult to achieve reliable (e.g., long-term operation or high self-starting capability) stretched-pulse mode-locking operation in our experiment due to the limited modulation depth of our CNT-SA (∼16%). Increasing the length of DCF (i.e., increase the GDD) would be a better choice which will be considered in the future due to the currently limited length of our HC-PCF.

4. Conclusion

In summary, we demonstrate a highly integrated all-fiber Er CPA system based on compression in HC-PCF. The influence of TOD on the pulse compression is experimentally investigated, in which a negative uncompensated TOD is able to reduce the accumulated nonlinear effects. The system could generate a relatively low pedestal 344-fs pulse with the energy of 25.1 nJ and the average power of 1.02 W after TOD optimization. Higher pump power leads to a decrease of pulse quality (i.e., larger pedestal and wider width) as a result of the excessive nonlinearities caused by a limited pulse stretching ratio in our CPA system. Such limitations can be overcome by using a much larger stretching ratio together with proper TOD management. Our architecture opens up new possibilities for building up a compact and completely fiber integrated high-performance Er CPA system.

References

[1] J. He, J. Miyazaki, N. Wang, H. Tsurui, and T. Kobayashi, "Biological imaging with nonlinear photothermal microscopy using a compact supercontinuum fiber laser source," *Opt. Express*, vol. 23, no. 8, pp. 9762–9771, 2015.
[2] M. Malinauskas *et al.*, "Ultrafast laser processing of materials: From science to industry," *Light: Sci., Appl., Rev.*, vol. 5, 2016, Paper e16133.
[3] M. E. Fermann and I. Hartl, "Ultrafast fiber laser technology," *IEEE J. Sel. Top. Quantum Electron.*, vol. 15, no. 1, pp. 191–206, Jan. 2009.
[4] I. Pavlov *et al.*, "Femtosecond laser written waveguides deep inside silicon," *Opt. Lett.*, vol. 42, no. 15, pp. 3028–3031, 2017.
[5] K. Plamann *et al.*, "Ultrashort pulse laser surgery of the cornea and the sclera," *J. Opt.*, vol. 12, no. 8, 2010, Art. no. 084002.
[6] J. Wang *et al.*, "Pulse dynamics in carbon nanotube mode-locked fiber lasers near zero cavity dispersion," *Opt. Express*, vol. 23, no. 8, pp. 9947–9958, 2015.
[7] I. R. Woodward and J. R. E. Kelleher, "2D saturable absorbers for fibre lasers," *Appl. Sci.*, vol. 5, no. 4, 2015.
[8] X. Li *et al.*, "Single-wall carbon nanotubes and graphene oxide-based saturable absorbers for low phase noise mode-locked fiber lasers," *Sci. Rep.*, vol. 6, no. 1, 2016, Art. no. 25266.
[9] B. Guo, "2D noncarbon materials-based nonlinear optical devices for ultrafast photonics [invited]," *Chin. Opt. Lett.*, vol. 16, no. 2, 2018, Art. no. 020004.
[10] W. Liu, M. Liu, Y. OuYang, H. Hou, M. Lei, and Z. Wei, "CVD-grown $MoSe_2$ with high modulation depth for ultrafast mode-locked erbium-doped fiber laser," *Nanotechnology*, vol. 29, no. 39, 2018, Art. no. 394002.

[11] D. Strickland and G. Mourou, "Compression of amplified chirped optical pulses," *Opt. Commun.*, vol. 56, no. 3, pp. 219–221, 1985.
[12] I. Pavlov, E. Ilbey, E. Dülgergil, A. Bayri, and F. Ö. Ilday, "High-power high-repetition-rate single-mode Er-Yb-doped fiber laser system," *Opt. Express*, vol. 20, no. 9, pp. 9471–9475, 2012.
[13] G. Sobon, P. R. Kaczmarek, D. Sliwinska, J. Sotor, and K. M. Abramski, "High-power fiber-based femtosecond CPA system at 1560 nm," *IEEE J. Sel. Top. Quantum Electron.*, vol. 20, no. 5, pp. 492–496, Sep/Oct. 2014.
[14] F. Morin, F. Druon, M. Hanna, and P. Georges, "Microjoule femtosecond fiber laser at 1.6 μm for corneal surgery applications," *Opt. Lett.*, vol. 34, no. 13, pp. 1991–1993, 2009.
[15] G. Sobon, P. Kaczmarek, A. Gluszek, J. Sotor, and K. M. Abramski, "μJ-level, kHz-repetition rate femtosecond fiber-CPA system at 1555 nm," *Opt. Commun.*, vol. 347, pp. 8–12, 2015.
[16] X. Peng *et al.*, "High efficiency, monolithic fiber chirped pulse amplification system for high energy femtosecond pulse generation," *Opt. Express*, vol. 21, no. 21, pp. 25440–25451, 2013.
[17] L. V. Kotov *et al.*, "Submicrojoule femtosecond erbium-doped fibre laser for the generation of dispersive waves at submicron wavelengths," *Quantum Electron.*, vol. 44, no. 5, pp. 458–464, 2014.
[18] P. Elahi, H. Kalaycıoğlu, H. Li, Ö. Akçaalan, and F. Ö. Ilday, "175 fs-long pulses from a high-power single-mode Er-doped fiber laser at 1550 nm," *Opt. Commun.*, vol. 403, pp. 381–384, 2017.
[19] X. Peng *et al.*, "Monolithic fiber chirped pulse amplification system for millijoule femtosecond pulse generation at 1.55 μm," *Opt. Express*, vol. 22, no. 3, pp. 2459–2464, 2014.
[20] J. C. Knight, J. Broeng, T. A. Birks, and P. S. J. Russell, "Photonic band gap guidance in optical fibers," *Science*, vol. 282, no. 5393, 1998, Art. no. 1476.
[21] D. G. Ouzounov *et al.*, "Generation of megawatt optical solitons in hollow-core photonic band-gap fibers," *Science*, vol. 301, no. 5640, 2003, Art. no. 1702.
[22] H. Lim and F. W. Wise, "Control of dispersion in a femtosecond ytterbium laser by use of hollow-core photonic bandgap fiber," *Opt. Express*, vol. 12, no. 10, pp. 2231–2235, 2004.
[23] J. Limpert, T. Schreiber, S. Nolte, H. Zellmer, and A. Tünnermann, "All fiber chirped-pulse amplification system based on compression in air-guiding photonic bandgap fiber," *Opt. Express*, vol. 11, no. 24, pp. 3332–3337, 2003.
[24] A. J. Verhoef *et al.*, "High peak-power monolithic femtosecond ytterbium fiber chirped pulse amplifier with a spliced-on hollow core fiber compressor," *Opt. Express*, vol. 22, no. 14, pp. 16759–16766, 2014.
[25] G. Imeshev, I. Hartl, and M. E. Fermann, "An optimized Er gain band all-fiber chirped pulse amplification system," *Opt. Express*, vol. 12, no. 26, pp. 6508–6514, 2004.
[26] A. Shirakawa, M. Tanisho, and K. Ueda, "Polarization-maintaining fiber pulse compressor by birefringent hollow-core photonic bandgap fiber," *Opt. Express*, vol. 14, no. 25, pp. 12039–12048, 2006.
[27] C. J. S. de Matos, J. R. Taylor, T. P. Hansen, K. P. Hansen, and J. Broeng, "All-fiber chirped pulse amplification using highly-dispersive air-core photonic bandgap fiber," *Opt. Express*, vol. 11, no. 22, pp. 2832–2837, 2003.
[28] C. J. S. de. Matos and J. R. Taylor, "Multi-kilowatt, all-fiber integrated chirped-pulse amplification system yielding 40$\times$ pulse compression using air-core fiber and conventional erbium-doped fiber amplifier," *Opt. Express*, vol. 12, no. 3, pp. 405–409, 2004.
[29] P. Hlubina, M. Kadulová, and D. Ciprian, "Spectral interferometry-based chromatic dispersion measurement of fibre including the zero-dispersion wavelength," *J. Eur. Opt. Soc. Rap. Public.*, vol. 7, 2012, Art. no. 12017.
[30] P. Ciąćka, A. Rampur, A. Heidt, T. Feurer, and M. Klimczak, "Dispersion measurement of ultra-high numerical aperture fibers covering thulium, holmium, and erbium emission wavelengths," *J. Opt. Soc. Am. B*, vol. 35, no. 6, pp. 1301–1307, 2018.
[31] G. M. Ponzo *et al.*, "Fast and broadband fiber dispersion measurement with dense wavelength sampling," *Opt. Express*, vol. 22, no. 1, pp. 943–953, 2014.
[32] L. Shah, Z. Liu, I. Hartl, G. Imeshev, G. C. Cho, and M. E. Fermann, "High energy femtosecond Yb cubicon fiber amplifier," *Opt. Express*, vol. 13, no. 12, pp. 4717–4722, 2005.
[33] S. Zhou, L. Kuznetsova, A. Chong, and F. W. Wise, "Compensation of nonlinear phase shifts with third-order dispersion in short-pulse fiber amplifiers," *Opt. Express*, vol. 13, no. 13, pp. 4869–4877, 2005.
[34] H. Song, B. Liu, L. Wen, C. Wang, and M. Hu, "Optimization of nonlinear compensation in a high-energy femtosecond fiber CPA system by negative TOD fiber," *IEEE Photon J.*, vol. 9, no. 2, Apr. 2017, Art. no. 3200110.
[35] L. Kuznetsova and F. W. Wise, "Scaling of femtosecond Yb-doped fiber amplifiers to tens of microjoule pulse energy via nonlinear chirped pulse amplification," *Opt. Lett.*, vol. 32, no. 18, pp. 2671–2673, 2007.